We are IntechOpen, the world's leading publisher of Open Access books Built by scientists, for scientists

6,900
Open access books available

185,000
International authors and editors

200M
Downloads

Our authors are among the

154
Countries delivered to

TOP 1%
most cited scientists

12.2%
Contributors from top 500 universities

CLARIVATE ANALYTICS
BOOK CITATION INDEX
INDEXED

WEB OF SCIENCE™

Selection of our books indexed in the Book Citation Index
in Web of Science™ Core Collection (BKCI)

Interested in publishing with us?
Contact book.department@intechopen.com

Numbers displayed above are based on latest data collected.
For more information visit www.intechopen.com

Preparation of Na⁺ Superionic Conductors by Crystallization of Glass

Toshinori Okura
Kogakuin University
Japan

1. Introduction

The use of glass-making processing is favorable for the fabrication of Na^+ conducting electrolyte tubes, which has been the key to the technological development of 1 MW Na/S secondary battery plants. However, the processing technique cannot be applied to well-known β- and β''-aluminas (e. g., $NaAl_{11}O_{17}$ and $NaAl_5O_8$) and Nasicons ($Na_{1+x}Zr_2P_{3-x}Si_xO_{12}$) because their high inclusion of Al_2O_3 or ZrO_2 brings about the inhomogeneous melting or crystallization from glasses. Alternatively, Nasicon-like glass-ceramics were synthesized using the composition with lower content of ZrO_2 ($mNa_2O \cdot xZrO_2 \cdot yP_2O_5 \cdot (100-m-x-y)SiO_2$ [m=20, 30 mol%]), however, the conductivities (σ) attained were, at most, as high as $\sigma_{300}=2\times10^{-2}$ S/cm at 300°C with the activation energies (E_a) of ca. 30 kJ/mol. These low conductivities were attributed to the crystallization of the poorly conductive rhombohedral phase in these Nasicon-like materials. $Na_5YSi_4O_{12}$ (N5), which comprises 12-$(SiO_4)^{4-}$-tetrahedra membered skeleton structure (Fig. 1), is another Na^+-superionic conductor with $\sigma_{300}=1\times10^{-1}$ S/cm and E_a=25 kJ/mol. A pioneering work on N5-type glass-ceramics has been performed by Banks *et al.* on the family of N5-type materials by substituting Y with Er, Gd or Sm. However, their results were not completely satisfactory because of the relatively lower conductivities of $\sigma_{300}<2\times10^{-2}$ S/cm than the reported values of N5. This discrepancy may possibly have arisen from the occurrence of a less conductive metastable phase during crystallization, as is discussed below.

Contrary to the results of Banks *et al.*, the present authors have produced glass-ceramics with $\sigma_{300}=1\times10^{-1}$ S/cm and E_a=20 kJ/mol, which were based on the phosphorus-containing N5-type materials discovered in the Na_2O-Y_2O_3-P_2O_5-SiO_2 system. These N5-type materials have been obtained, as well as $Na_3YSi_3O_9$ (N3)-type materials, with the composition formula originally derived for N3-type solid solutions and expressed as follows,

$$Na_{3+3x-y}Y_{1-x}P_ySi_{3-y}O_9 \ (x<0.6, y<0.5) \tag{1}$$
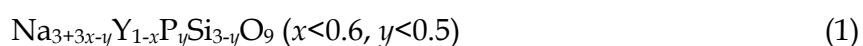
With the aim of searching for more conductive glass-ceramic N5-type materials, the verification of the validity of the generalized composition formula

$$Na_{3+3x-y}R_{1-x}P_ySi_{3-y}O_9 \tag{2}$$

for the synthesis of other kinds of rare earth N5-type glass-ceramics was studied first. Formula 2 is rewritten with formula 3 according to the formula N5.

$$Na_{4(3+3x-y)/3}Y_{4(1-x)/3}P_{4y/3}Si_{4(3-y)/3}O_{12} \tag{3}$$
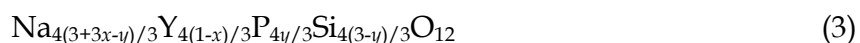
In relation to previous works, formula 2 was employed in this work, and formula 3 is referred to in the results. The trivalent ions employed here for R^{3+} were Sc^{3+}, In^{3+}, Er^{3+}, Gd^{3+}, Sm^{3+}, Eu^{3+}, Nd^{3+} and La^{3+} as well as Y^{3+}. These results are to be interpreted in terms of the effect of the rare earth ions on the crystallization of N5-type phase in glasses.
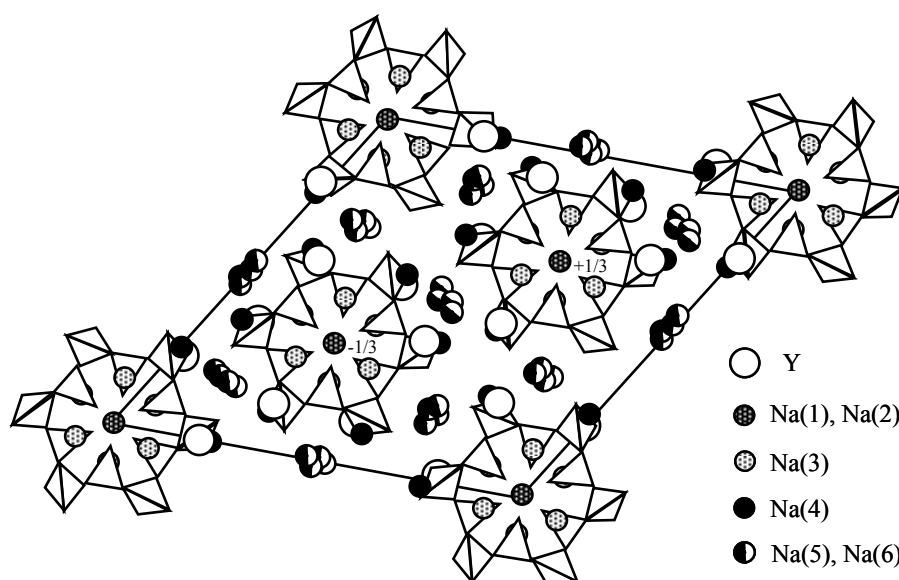

Fig. 1. Crystal Structure of $Na_5YSi_4O_{12}$. Projection of the $Na_5YSi_4O_{12}$ Structure on (100).

In the course of the fundamental studies on glass-ceramic $Na_{3+3x-y}R_{1-x}P_ySi_{3-y}O_9$, we have interestingly found the crystallization of those N3- and $Na_9YSi_6O_{18}$ (N9)-type phases as the precursors in the glasses. These are the analogues to the silicates N3 and N9 and therefore are the same members of the family of $Na_{24-3x}Y_xSi_{12}O_{36}$ as N5. Although we had also successfully synthesized those materials by the solid-state reactions of powders with the above composition of various sets of the parameters x and y, the metastability of those precursor phases had not been noticed in the synthesis. It has been observed that such precursor phases were transformed to the Na^+-superionic conducting phase on specimens with appropriate sets of x and y. The present paper will deal with the thermodynamic and kinetic study on the phase transformation of metastable phases to the stable phase with Na^+-superionic conductivity. The superiority of our present materials to the other silicate N5 will also be detailed based on the kinetic results.

The microstructure of a glass-ceramic, including neck growth among grains as well as grain size, is generally affected by the crystallization process. As the above mentioned devices utilize dc conduction properties of Na^+-superionic conductors, another aim was to study the microstructural effects on the conduction properties of a whole glass-ceramic. Special attention was paid to the analysis of grain boundary properties using the Na_2O-Y_2O_3-P_2O_5-SiO_2 system. For the analysis of grain boundary properties, as will be discussed below, composition dependences of the conductivity of sodium silico-phosphate glasses containing Y_2O_3 were also studied in the Na_2O-Y_2O_3-P_2O_5-SiO_2 system. For convenience, the present materials are abbreviated as NaRPSi taken from the initials of the Na_2O-R_2O_3-P_2O_5-SiO_2 system.

2. Materials

2.1 Preparation of glasses and glass-ceramics

Precursor glasses were prepared from reagent-grade oxides of anhydrous Na_2CO_3, R_2O_3 (R=Y, Sc, In, Er, Gd, Sm, Eu, Nd, La), $NH_4H_2PO_4$ and SiO_2; the mechanically mixed powders according to formula 2 or appropriate compositions shown below were melted at 1350°C for 1 h after calcinations at 900°C for 1 h. The melts were quickly poured into a cylindrical graphite, then annealed at 500°C for 3 h, giving NaRPSi glasses. The composition parameters studied were in the range of 0.2<x<0.6 and 0<y<0.5 of formula 2. As shown below, grain boundary conduction properties are discussed in relation to the properties of glasses. For the evaluation of the composition dependence of conductivity in Na$^+$ conducting glasses, various sodium yttrium silico-phosphate glass specimens with different atomic ratios of [Na]/[P+Si] and [Na]/[Y] were also prepared.

Crystallization was carried out according to the previous report; bulk glasses were heated with an increasing rate of 75°C/h to a temperature above ca. 50°C of the glass transition point, which had been determined in advance by differential thermal analysis (DTA). This pretreatment was done in order to obtain homogeneous nucleation. After the annealing for 1 h, specimens were heated at temperatures of 800 to 1100°C, depending on the composition, for 0.5 to 72 h, thereafter slowly cooled in a furnace with a decreasing rate of 150°C/h to room temperature. These quenched glasses or glass-ceramic specimens were polished down with 0.5 μm diamond paste, thereafter subjected to the conductivity measurements.

2.2 Measurements and characterization

Ionic conductivities were measured by the complex impedance method on cylindrical glasses or glass-ceramics of typically 15 mm in diameter and 2 mm in thickness. Electrodes were prepared by sputtering of gold on polished surfaces. The applied ac field ranged from 5 to 10 MHz in frequency. The temperature dependence of the conductivity was measured in a similar way at several temperatures ranging from room temperature to 350°C. The complex impedance or admittance loci of glass and glass-ceramics were analyzed by an equivalent circuit (Fig. 2), which was experimentally found to comprise one and two semicircles in NaRPSi glasses and glass-ceramics, respectively. The two intercepting points on the real axis are interpreted as the resistance of crystallized grains ($R_{G(c)}$) and the total resistance of grains and remaining glassy grain boundaries ($R_{GB(g)}$). Assume the complex admittance diagram shown in Fig. 3, where the parameters L_1 and L_2 are set here as the radii of the two arcs 1 and 2. Those parameters are related to one another as the following:

$$L_1 \propto 1/(R_{G(c)} + R_{GB(g)}) \tag{4}$$

and

$$L_2 \propto (1/R_{G(c)}) - 1/(R_{G(c)} + R_{GB(g)}) \tag{5}$$

Then,

$$L_2/L_1 = R_{GB(g)}/R_{G(c)} \tag{6}$$

Therefore, in an ideal grass-ceramic where residual glass would have negligible influence on the total, arc 2 would be much smaller than arc 1, since $L_2/L_1 \rightarrow 0$.

Crystalline phases of glass-ceramic specimens were identified by X-ray diffraction (XRD) method. The lattice parameters of the N5-type hexagonal unit cell were calculated by a least-squares method using the XRD peaks of (054), (044), (134), (440) and (024). Glass-ceramics of Y^{3+}-contained NaRPSi were subjected to scanning (SEM) and transmission electron microscope (TEM) for microstructural analysis. Electron diffraction and compositional analyses were also performed to characterize the structure of the grain boundary.

For the description of a specific NaRPSi, R of the term will be replaced, respectively, with Y, Sc, In, Er, Gd, Sm, Eu, Nd and La as NaYPSi, NaScPSi, NaInPSi, NaErPSi, NaGdPSi, NaSmPSi, NaEuPSi, NaNdPSi and NaLaPSi for Y_2O_3, Sc_2O_3, In_2O_3, Er_2O_3, Gd_2O_3, Sm_2O_3., Eu_2O_3, Nd_2O_3 and La_2O_3.

3. Thermodynamic and kinetic study on the phase transformation

3.1 Composition dependence of precursor and high temperature stable phases

Fig. 4 shows the composition dependence of both the precursor phases and the high temperature stable phases of glass-ceramic NaYPSi on the maps of phosphorus-yttrium (P-Y, Fig. 4(a)), yttrium-sodium (Y-Na, Fig. 4(b)) and phosphorus-sodium (P-Na, Fig. 4(c)), where the variables on the abscissas and ordinals are expressed with the composition parameters $1-x$, y and $3+3x-y$ for yttrium, phosphorus and sodium, respectively. As reported before, N3- and N9-type NaYPSi glass-ceramics can be crystallized as the high-temperature stable phases at the regions of higher [Y] ($1-x>$ca. 0.8) and rather lower [Y] ($1-x<$ca. 0.55), respectively, in the [Y]-[P] relation.
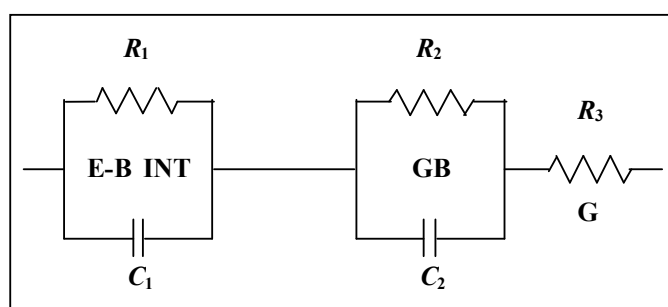

Fig. 2. Equivalent circuit employed for the admittance analysis.

E-B INT, GB, and G represent the electrode-bulk interface, grain-boundaries and grains, respectively, and (R_1, C_1), (R_2, C_2), and R_3 are their resistances and capacitances.

Concerning the precursor phases, only either N3- or N9-type NaYPSi was found in any composition, while N5-type NaYPSi was difficult to crystallize from glasses at low temperatures. It is also seen in the [P]-[Y] map (Fig. 4(a)) that, under a given phosphorus content ([P]<0.6) a composition with higher content of yttrium gives N3-type NaYPSi (○) as the precursor phase, while lower [Y] content results in N9-type phase (open square). The values of [Y] dividing the regions allowed for N3- and N9-type NaYPSi glass-ceramics decreased with increasing [P], and the boundary seems to locate slightly apart from the deduced line of [Y]=0.75-0.5[P] shown with the solid line. Around the boundary region N5-type NaYPSi can be obtained as the stable phase at high temperatures (solid marks of circle or square). In the [Y]-[Na] or [P]-[Na] relations (Figs. 4(b) and 4(c)), the region where
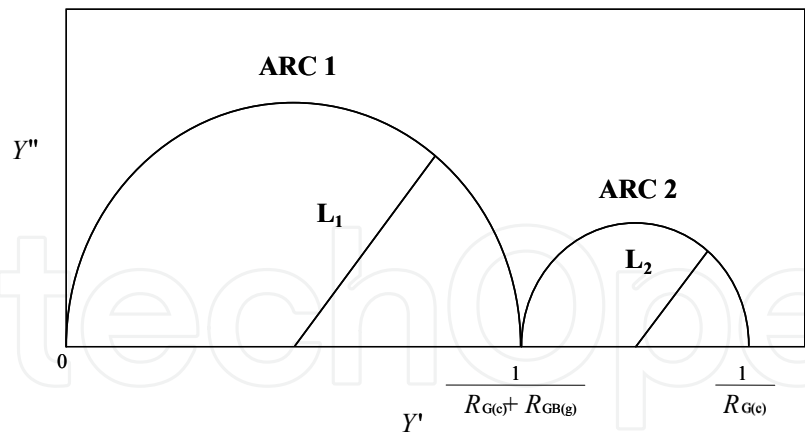
Fig. 3. An idealized diagram of complex admittance for glass-ceramics, in which arc 1 (ARC 1) and arc 2 (ARC 2) are related to the crystallized grains (G(c)) and remaining glasses (GB(g)). L$_1$, L$_2$, $R_{G(c)}$, and $R_{GB(g)}$ are, respectively, the radii of arcs 1 and 2, the resistances of G(c) and GB(g).
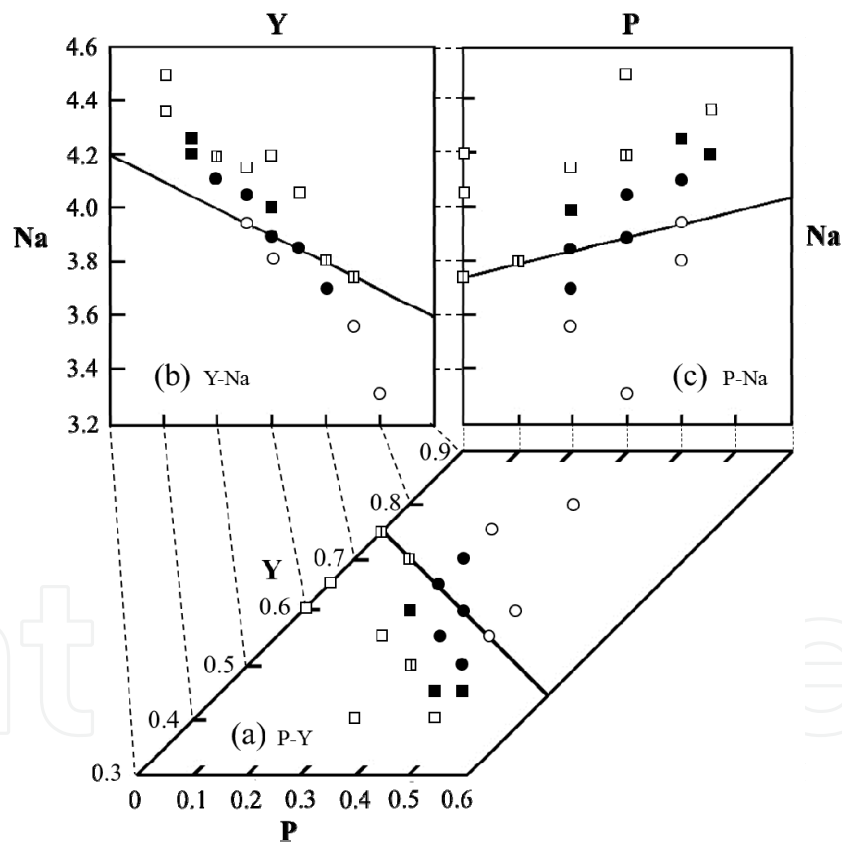

Fig. 4. Composition dependence of precursor (*pp*) and high temperature-stable phases (*sp*) of glass-ceramic NaRPSi on P-Y (a), Y-Na (b) and P-Na (c) maps, where precursor phases N3 and N9 are shown with *circles* and *squares*, respectively. High temperature-stable phases are shown in such a way that solid marks means that N5-NaRSi is the stable, while *open marks* indicate that the precursor phases are also stable even at high temperatures. Mixed phases are also shown: *open circle* pp = sp = N3; *filled circle* pp = N3, sp = N5; *open square* pp = sp = N9; *filled circle* pp = N9, sp = N5; *open split square* pp = N9, sp = N9 + N5

N5-type NaYPSi can be found as the high-temperature stable phase is found under ca. 3.6<[Na]<4.3. The effect of sodium content seems insignificant, because the value of [Na] is subordinately determined as [Na]=6-3[Y]-[P] (=3+3x-y) depending on the contents of both yttrium and phosphorus.

The above results may suggest that the [P]-[Y] relation dominates the region which is allowed for each NaYPSi at high temperatures. Considering this inference, we calculated the products of [P]×[Y] for all of the specimens. The values of [P]×[Y] were as follows (shown in Fig. 5); 0.16-0.25 for single phase N3-type NaYPSi, 0.14 for mixed phases of N3- and N5-type NaYPSi, 0.12-0.20 for single phase N5-type NaYPSi, 0-0.14 for the mixed phases of N5- and N9-type NaYPSi, and 0-0.17 for single phase N9-type NaYPSi, respectively. It was therefore deduced (Fig. 5) that the free energy of formation (ΔG_f) of N9-type NaYPSi would be the lowest in a lower region of [P]×[Y], N5-type NaYPSi may have the lowest ΔG_f in a medium [P]×[Y] region, and higher [P]×[Y] would lower ΔG_f of N3-type NaYPSi.

For a specimen in which N5-type NaYPSi is the stable phase at high temperatures, the aspect such as Fig. 6a would be illustrated in that ΔG of N3- or N9-type NaYPSi would be much smaller than that of N5-type NaYPSi near the crystallization temperature (T_c), and the value of N5-type NaYPSi would be lowered much less than of the two. Fig. 6b indicates the aspect that ΔG or N3- or N9-type NaYPSi stable.
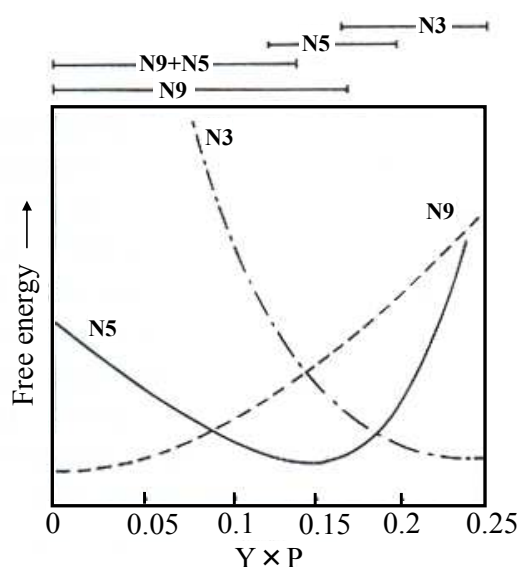

Fig. 5. Schematic figure of composition ([Y]×[P]) dependence of free energy of N5-, N3- and N9-type NaYPSi.
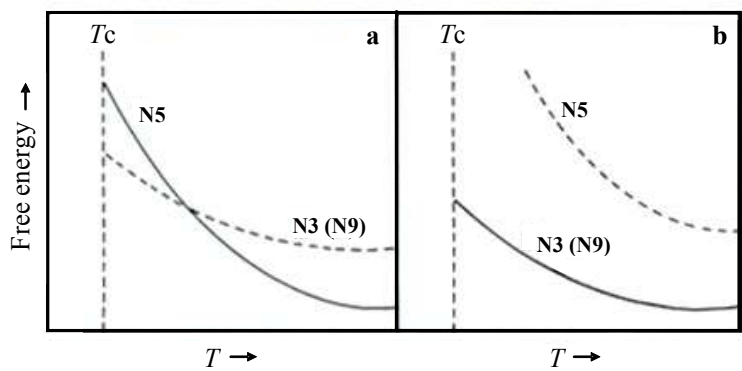
Fig. 6. Schematic figures of temperature dependence of free energy change of N5- and N3- or N9- type NaYPSi in the cases assuming N5- (a) and N3- (b) or N9-type (b) NaYPSi as the high temperature-stable phase, where Tc is the crystallization temperature.
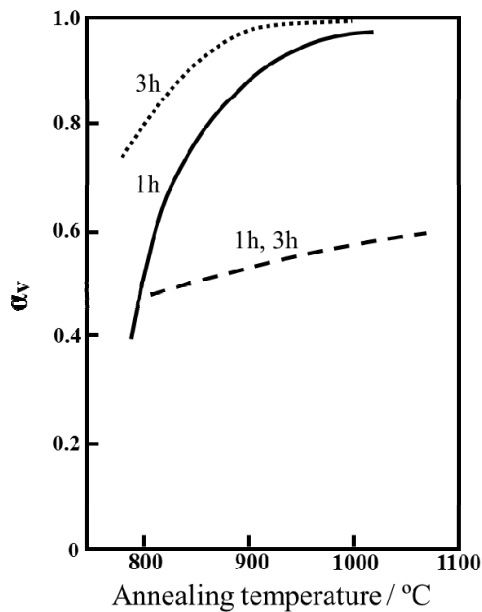

Fig. 7. Comparison of phase transformation rate (α_v) between specimens $Na_{3.9}Y_{0.6}P_{0.3}Si_{2.7}O_9$ (1h-annealing: (○); 3h-annealing: (●)) and $Na_{3.75}Y_{0.65}P_{0.3}Si_{2.7}O_9$ (1h-annealing: (□), 3h-annealing: (■)).

3.2 Kinetic effects of composition on the phase transformation

The kinetic effects of composition on the phase transformation are shown in Fig. 7, which compares the phase transformation rates of specimens $Na_{3.9}Y_{0.6}P_{0.3}Si_{2.7}O_9$ and $Na_{3.75}Y_{0.65}P_{0.3}Si_{2.7}O_9$. The transformation rate (α_v) of a precursor phase to the stable N5 phase was determined as the weight ratio of N5-type NaYPSi in a glass-ceramic specimen. The value of α_v was experimentally obtained from the relationship of weight ratio to XRD intensity ratio, which relationship had been made previously by XRD intensity measurement on specimens with given weight ratio of N5-type NaYPSi to metastable phases. It is seen that the composition $Na_{3.9}Y_{0.6}P_{0.3}Si_{2.7}O_9$ is superior to the other, for the N5 single phase NaYPSi was difficult to obtain in the latter specimen. In specimen

$Na_{3.9}Y_{0.6}P_{0.3}Si_{2.7}O_9$ a glass-ceramic of N5 single phase NaYPSi was easily obtained at a temperature higher than 900°C for only three hours. The composition $Na_{3.75}Y_{0.75}Si_3O_9$ (or $Na_5YSi_4O_{12}$) was inferior in the same meaning.
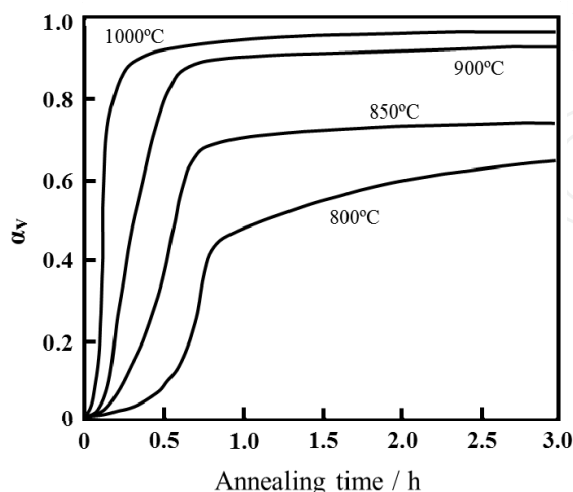
Fig. 8. Phase transformation rate (α_v) of N3- to N5-type NaYPSi on the specimen $Na_{3.9}Y_{0.6}P_{0.3}Si_{2.7}O_9$.

Fig. 8 shows the kinetic characteristics of phase transformation of the metastable phase of N3- to N5-type NaYPSi of specimen $Na_{3.9}Y_{0.6}P_{0.3}Si_{2.7}O_9$ at various temperatures. The transition rates, α_v, of the silicophosphate NaYPSi were much higher than those of the $Na_{3.75}Y_{0.75}Si_3O_9$ silicate material.

The results shown were analyzed with the Avrami empirical equation, $\alpha_v = 1 - \exp(-kt^n)$, where k is the rate constant, and n is a constant. The data on α_v obtained at the initial and intermediate stages gave a linear relationship between $\ln(\ln(1-\alpha_v)^{-1})$ and $\ln(t)$ with a correlation coefficient of more than 0.99. The Avrami parameter and rate constants obtained are summarized in Table 1. Based on the Arrhenius relationship (Fig. 9), $k = A\exp(-E_v/RT)$ with E_v as the activation energy and constants A and R, on those k values which increased with increasing temperature, we obtained an activation energy of 1.2×10^3 kJ/mol, suggesting that the phase transformation can be rather difficult to take place. An addition of phosphorus and the excess sodium seem effective to the promotion of the phase transformation.

4. Microstructural effects on conduction properties

4.1 Crystallization and phase diagram

As expected from the previously reported results on NaYPSi, the crystallization of the superionic conducting N5-type phase took place, depending both on the contents of [R] and [P], at temperatures of 800 to 1000°C in most NaRPSi glasses of Er to Sm except for scandium and lanthanum NaRPSi glasses. The N5 single phase region was wider for NaRPSi of smaller R, but was limited at the [P]≈0 region. The effect of phosphorus substitution for Si is important in the crystallization of N5-type phase. The composition 7

$$Na_{3.9}R_{0.6}P_{0.3}Si_{2.7}O_9 \qquad (7)$$

was experimentally shown as the most appropriate composition for the crystallization of N5-type phase.

Anneling temp. (K)	Avrami modulus n	ln k
1073	2.61	-20.7
1123	1.94	-14.6
1173	1.39	-9.54
1223	0.75	-4.41

Table 1. Kinetic parameters of phase-transformation of N3- to N5-type NaYPSi of Na$_{3.9}$R$_{0.6}$Si$_{2.7}$O$_9$.
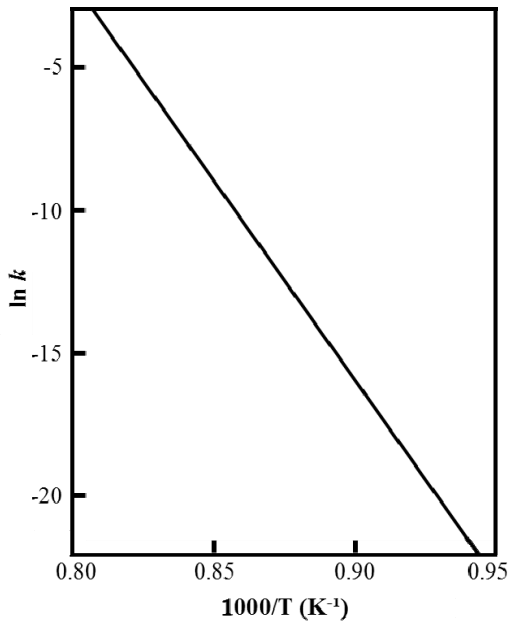

Fig. 9. Arrhenius-type plot of ln k with 1000/T of specimen Na$_{3.9}$Y$_{0.6}$Si$_{2.7}$O$_9$.

The relationship between the ionic radius of R^{3+} (r_R) and the hexagonal lattice parameters of N5-type single phase is consistent with the previous report on Na$_5$RSi$_4$O$_{12}$ (R=Sc-Sm) in the tendency that both lattice parameters increased with increasing r_R. The elongation of these lattice axes is attributed to the octahedral coordination of R^{3+} with the O^{2-} of SiO$_4$- or PO$_4$-tetrahedra of the 12-membered rings. The local structure around R^{3+} ions is to be further discussed below in relation to conduction properties. On the formation of N5-type single phase, the incorporation of excess sodium ions [4(3+3x-y)/3-5=(12x-4y-3)/3 in composition 3] and substitution of rare earth ions [1-4(1-x)/3=(4x-1)/3] must be accounted for in view of N5-type crystal structure.

Banks et al. have reported the values of σ$_{300}$ as 5×10^{-3} to 1×10^{-2} S/cm for glass-ceramic Na$_5$RSi$_4$O$_{12}$ (R=Er, Y, Gd, Sm), which are as low as those of the mixed phase NaRPSi specimens. The single phase N5-type glass-ceramic was not obtained in the present work. Based on the above crystallization analysis, their glass-ceramic specimens are reasonably

considered to suffer from phase inhomogeneity brought about by insufficient annealing. The formation of N5-type structure from the precursor glasses is a matter of crystallization kinetics, since single-phase N5 has been synthesized in single crystal or polycrystalline form based on the composition of N5. It is noted here that the precursor phases identified were N3- or N9-type. Both N3 and N9 are considered to form iso-structural with $Ca_3Al_2O_6$ to be comprised of the skeleton structure of 6-membered SiO_4-tetrahedra rings. It is generally known that phosphorus pentoxide acts as nucleating agent in the formation of glass-ceramics. It is therefore presumed at present that the substitution of an asymmetric PO_4-tetrahedron has the weakening effect on the bonding of the skeleton structure of 6-membered SiO_4-tetrahedra rings, resulting in the tendency to form the stable 12-membered structure.
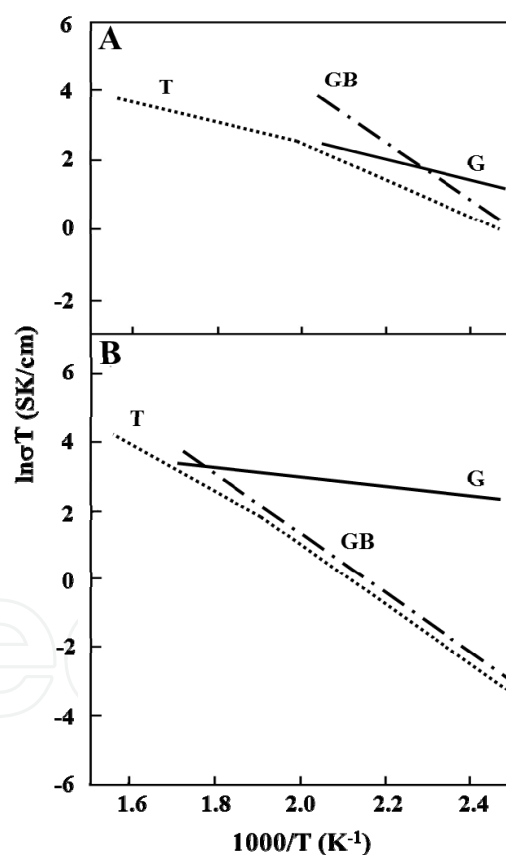

Fig. 10. The Arrhenius plots of the conductivities of grains (G), grain boundaries (GB) and the total bulk (T) of the glass-ceramic $Na_{3.9}Y_{0.6}P_{0.3}Si_{2.7}O_9$ (A) and $Na_{3.9}P_{0.3}Sm_{0.6}Si_{2.7}O_9$ (B).

R^{3+} (ions)	E_a kJ/mol	Conductivity (σ_{300}) S/cm	Crystalline phase
Sc	35.3	3.2×10^{-3}	N5-type + unknown
In	39.8	3.1×10^{-3}	N5-type + unknown
Er	26.9	3.6×10^{-2}	N5-type
Y	26.6	6.6×10^{-2}	N5-type
Gd	23.0	1.3×10^{-1}	N5-type
Eu	24.4	5.2×10^{-2}	N5-type
Sm	20.9	6.3×10^{-2}	N5-type
Nd	55.1	2.2×10^{-5}	Unknown
La	57.8	1.6×10^{-4}	Unknown

Table 2. Conduction properties of various NaRPSi glass-ceramics with composition Na$_{3.9}$R$_{0.6}$Si$_{2.7}$O$_9$.

4.2 Conduction properties of crystalline grains

The complex impedances and admittances of the measured NaRPSi glass-ceramics consisted of two semicircles below 300°C. The two intercepting points on the real axis are interpreted as the resistance of crystallized grains (R_G) and the total resistance of grains and remaining glassy grain boundaries (R_{GB}). Shown in Fig. 10 are examples of the temperature dependence Arrhenius plots made on the basis of the calculated conductivity values of grains and grain boundaries of the glass-ceramic NaYPSi (Na$_{3.9}$Y$_{0.6}$P$_{0.3}$Si$_{2.7}$O$_9$) and NaSmPSi (Na$_{3.9}$Sm$_{0.6}$P$_{0.3}$Si$_{2.7}$O$_9$), in which the geometrical ratios of thickness to surface area for grains were also used for convenience for those of grain boundaries because of their undefinable shapes. Table 2 summarizes the measured conductivities (σ_{300}) and the calculated activation energies (E_a) assigned for grains of the glass-ceramics with composition 7 of Sc to La, regardless of whether their crystalline phases are N5-type or not. The conductivities, σ_{300}, of single-phase NaRPSi specimens of Er to Sc range from 4×10^{-2} to 1×10^{-1} S/cm; in accordance the E_a falls in the range of 23 to 27 kJ/mol. In contrast, the mixed phase NaRPSi of Sc and In showed much smaller σ_{300} of 3×10^{-3} with an E_a of 35 to 40 kJ/mol, while non-NaRPSi glass-ceramics with unknown or mixed phases showed much lower conductivities of 1×10^{-5} to 1×10^{-4} S/cm with an E_a of 55 to 58 kJ/mol.

The tendency of the conduction properties in single-phase NaRPSi specimens is consistent with the reported result measured on the corresponding polycrystalline Na$_5$RSi$_4$O$_{12}$; σ increased with increasing r_R. The previous works have proposed a mechanism that rare earth ions, octahedrally coordinated with the non-bridging oxide ions of the 12-membered rings of silica tetrahedra, work to expand the conduction paths for Na$^+$ ions along the c-axis, which can explain the observed dependence of E_a on r_R in this work.

4.3 Structure and conduction properties of grain boundaries

As R_{GB} decreases rapidly with increasing temperature because of high $(E_a)_{GB}$ to a comparable value with R_G at 300°C (Fig. 10), the total conductivities (R_G+R_{GB}) are dominated by grain boundary conductivity. The grain size-dependence of σ_{300} is therefore explained by the decrease in the number of poorly conductive grain boundaries with increasing grain size.

The conduction properties of grain boundaries were strongly dependent on the annealing conditions, although those of the grains were little changed by annealing temperature and time. Glass-ceramics are generally composites consisting of crystallized grains and small amounts of residual glass (<1%). To compare the properties of grain boundaries with those of glasses, the conduction properties of sodium yttrium silicophosphate glasses with various compositions were measured. Unlike glass-ceramics the impedance loci of glasses were comprised of one arc, which indicates that there is no polarization arising from microstructural inhomogeneity. Based on the intercepting points on the horizontal axis, the composition dependence of conduction properties of σ_{300} and E_a were evaluated. The value of σ_{300} ranged from 1×10^{-4} to 5×10^{-3} S/cm and E_a increased from 53 to 67 kJ/mol with [Na] or [Na]/[Y]. These results are also in good agreement with those reported for the glasses in the Na_2O-Y_2O_3-SiO_2 system. The values of $(E_a)_{GB}$ of the specimens annealed below 950°C for shorter times correspond to those in the range of glasses, strongly suggesting that their grain boundaries are a glassy matrix. The above mentioned dependence of $(E_a)_{GB}$ on $[Na_2O]$ is explained by the well-known tendency that the conduction properties of glasses are improved by increasing $[Na_2O]$, which provides the increase of carrier Na^+ ions. The ratio of [Na]/[Y] is also an important parameter for the conduction properties, showing an effect on the conduction properties similar to $[Na_2O]$.

In order to identify the structure of the grain boundaries of the specimen ($Na_{3.9}Y_{0.6}P_{0.3}Si_{2.7}O_9$) annealed at 800°C for 0.5 h, TEM analysis was performed both on grains and grain boundaries. The results show clear electron diffraction on grains, while not on grain boundaries. This fact confirms that the grain boundaries are amorphous. Compositional analyses were also performed, however, [Na] was difficult to determine because of the evaporation by electron ablation. It was also observed that the glassy phase was condensed at triple points enclosed by grains, and that neck growth among the grains was well developed. Thus, it is reasonable to consider that the grain boundaries annealed at lower temperatures are amorphous, while those annealed at higher temperatures for longer periods of time are poorly conductive crystalline compounds in the specimens.

5. Recent research on conductive improvement and structural control of glass-ceramic Na^+ superionic conductors

5.1 Preparation of crack free $Na_5YSi_4O_{12}$-type glass-ceramics containing the largest Sm^{3+} ions: Crystallization condition and ionic conductivity

Glass-ceramics of the phosphorus containing N5-type Na^+ superionic conductors have been developed by crystallization of glasses with the composition formula 2. The R elements have a significant effect on the crystallization of glasses, as well as on the conduction properties. To date, polycrystalline N5-type NaRPSi has been obtained with Sc, Y, Gd or Sm as the R element. The ionic radius of R (sixfold oxygen coordinated R) has been expected to have a significant effect on the crystallization of the phase. The reported results on the silicate ceramics show that the conductivity of the N5-type NaRPSi increases with increasing ionic radius of R, giving the order NaSmPSi>NaGdPSi>NaYPSi>NaScPSi. It can be expected that NaSmPSi is the most conductive. However, this order was not always true in glass-ceramics. Although most of the NaRPSi compounds were obtained as crack free bulky glass-ceramics (15 mm in diameter, 5 mm in thickness), NaSmPSi was difficult to prevent from cracking during crystallization. It was found that crack free NaGdPSi with larger Gd^{3+} ions was the

most conductive; however, NaSmPSi with the largest Sm^{3+} ions was less conductive than NaYPSi with medium Y^{3+} ions. In the present study, the N5-type NaSmPSi ionic conductors were prepared by crystallization of glasses. The optimum conditions for crystallization were discussed with reference to the conduction properties and the preparation of crack free N5-type glass-ceramic NaSmPSi.

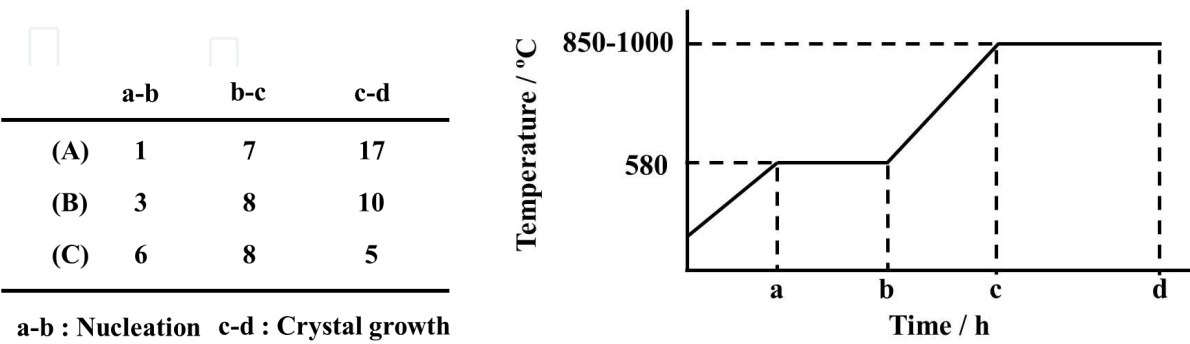|	a-b	b-c	c-d
(A)	1	7	17
(B)	3	8	10
(C)	6	8	5

a-b : Nucleation   c-d : Crystal growth

Fig. 11. Program of temperature and time for the production of NaSmPSi glass-ceramics.

Samples were prepared according to the chemical formula mentioned above of Na$_{3+3x-y}$Sm$_{1-x}$P$_y$Si$_{3-y}$O$_9$. The temperatures employed for nucleation and crystallization of glass specimens were also determined by the results of DTA analysis. Fig. 11 shows the program of temperature and time for the production of glass-ceramic NaSmPSi employed in the present work. The N5-type NaSmPSi ionic conductors were successfully produced by crystallization of glasses. Although the glass samples heated by the program pattern (A) shown in Fig. 11 broke during crystallization and the glass-ceramic NaSmPSi obtained by the pattern (B) was difficult to prevent from cracking during crystallization, most of the NaSmPSi compounds by the pattern (C) were obtained as crack free bulky glass-ceramics (the glass samples broke during crystallization when heating time for crystallization was over 5 h). Fig. 12 shows the phase-composition diagram of samples crystallized at 900°C by the pattern (C). The crystallization of the N5 single-phase glass-ceramic NaSmPSi was dependent strongly on the concentrations of both [R] and [P] (or x and y in the composition parameters) and the temperature for crystallization of glass specimens. Fig. 13 shows SEM photograph of microstructure of specimen with the Na$_{3.9}$Sm$_{0.6}$P$_{0.3}$Si$_{2.7}$O$_9$ composition heated at 900°C by the pattern (C). The grain size of the specimen was about 3-5 μm. The state of grain growth is promoted with increase of heating temperature and heating time for crystallization. Although grain growth may cause high conductivity, it was difficult to prevent the sample heated for a long time from cracking during crystallization. Studies are underway to produce a crack free sample. Conduction properties were measured by the ac two-probe method on cylindrical glass-ceramics of typically 15 mm in diameter and 2 mm in thickness with an LF impedance analyzer. Electrodes were prepared by sputtering of gold on polished surfaces. The applied ac field ranged from 5 to 10 MHz in frequency. The temperature dependence of the conductivity was measured in a similar way at several temperatures ranging from room temperature to 350°C. Table 3 summarizes the conduction properties of the N5-type glass-ceramic NaSmPSi specimens. It was found that NaSmPSi containing the largest Sm^{3+} ions was less conductive than NaYPSi with medium Y^{3+} ions as the grain sizes of the presented specimens were very small.
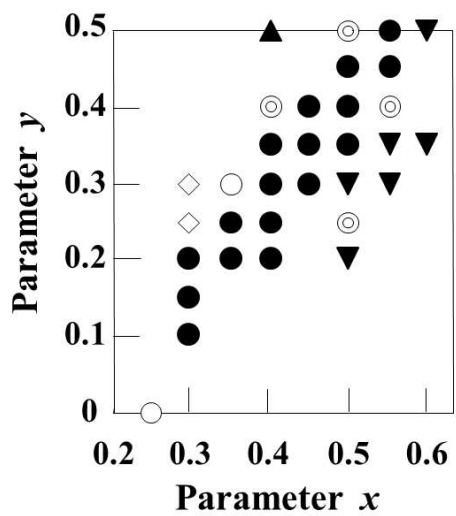
Fig. 12. The diagram of phase-composition of NaSmPSi glass-ceramics crystallized at 900°C.
● $Na_5YSi_4O_{12}$ (N5) type, ▲ $Na_3YSi_3O_9$ (N3) type, ▼ $Na_9RSi_6O_{18}$ (N9) type
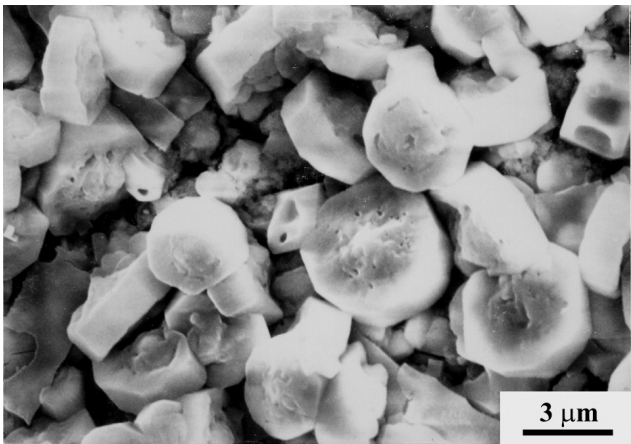○ N5+N3, ◎ N5+N9, ◇ N3+N9

Fig. 13. SEM photograph of the specimen with $Na_{3.9}Sm_{0.6}P_{0.3}Si_{2.7}O_9$ composition heated at 900°C by the pattern (C).

Mix proportion		σ_{300}	E_a / kJ·mol^{-1}		
x	y	/ 10^{-1} S·cm^{-1}	T	G	G. B.
0.40	0.30	0.238	27.6	17.9	51.4
0.45	0.40	0.408	30.4	18.8	95.7
0.50	0.35	0.352	19.5	15.8	
0.50	0.40	0.478	29.3	16.6	-------

σ_{300} : conductivity at 300 °C

E_a : activation energy (T : total G : grain G. B. : grain boundary)

Table 3. Conduction properties of N5-type NaSmPSi glass-ceramics.
Heat-treatment: 900°C, 5 h

5.2 Composition control of silico-phosphate glass-ceramics

5.2.1 Ionic conductivities of Nasicon-type glass-ceramic superionic conductors in the system Na$_2$O-Y$_2$O$_3$-XO$_2$-SiO$_2$ (X=Ti, Ge, Te)

Our phosphorus containing compositions have been confirmed superior to the mother composition of Na$_5$RSi$_4$O$_{12}$, especially in the production of the single-phase glass-ceramics. Considering the inference, our main work has recently been focused on the synthesis of various glass-ceramics with single-phase Na$_5$RSi$_4$O$_{12}$. In the present study, the glass-ceramics of the titanium-, germanium- or tellurium-containing Na$_5$RSi$_4$O$_{12}$-type (R=Y) Na$^+$-superionic conductors (N5YXS) from the glasses with the composition Na$_{3+3x}$Y$_{1-x}$X$_y$Si$_{3-y}$O$_9$ (X=Ti; NYTiS, Ge; NYGeS, X=Te; NYTeS) were prepared, and the effects of X elements on the separation of the phase and the microstructural effects on the conduction properties of glass-ceramics were discussed.

The glass-ceramics have been obtained under the appropriate sets of the parameters x and y of the composition formula Na$_{3+3x}$Y$_{1-x}$X$_y$Si$_{3-y}$O$_9$ ranging in x=0.1~0.55 and y=0.1~0.45. The precursor glasses were made by melting stoichiometric mixtures of reagent-grade powders of anhydrous Na$_2$CO$_3$, Y$_2$O$_3$, (TiO$_2$, GeO$_2$ or TeO$_2$) and SiO$_2$ at 1300~1400°C for 1 h, followed by annealing for several hours at an optimum temperature. The N5YXS ionic conductors were successfully produced by crystallization of glasses. Figs. 14, 15 and 16 show the diagrams of phase-composition-crystallization temperature of NYTiS, NYGeS and NYTeS glass-ceramics, respectively. The phase formed was dependent on composition and crystallization temperature. N5YTiS, N5YGeS and N5YTeS are obtained as a stable phase at high-temperatures. The crystallization of N5 single phase is strongly dependent both on the contents of yttrium and (titanium, germanium or tellurium) ions (or the values x and y correspond to the composition parameters in Na$_{3+3x}$Y$_{1-x}$X$_y$Si$_{3-y}$O$_9$). N3 and N9 phases can be crystallized as the high-temperature stable phases at the regions of higher [Y] and rather lower [Y], respectively. The combination of x and y was most varied in N5YGeS and more limited in the order of N5YTeS>N5YTiS. Table 4 summarizes the conduction properties of the N5 glass-ceramics with Na$_{3.6}$Y$_{0.8}$Ti$_{0.2}$Si$_{2.8}$O$_9$, Na$_{4.2}$Y$_{0.6}$Ge$_{0.3}$Si$_{2.7}$O$_9$ and Na$_{4.2}$Y$_{0.6}$Te$_{0.3}$Si$_{2.7}$O$_9$ compositions. Their conductivities and activation energies are of the order of 10^{-2} S/cm at 300°C and of 15 to 24 kJ/mol, respectively. The conductivity decreases giving the order N5YGeS>N5YTeS>N5YTiS. It is considered that this order corresponds to the N5 single phase region.
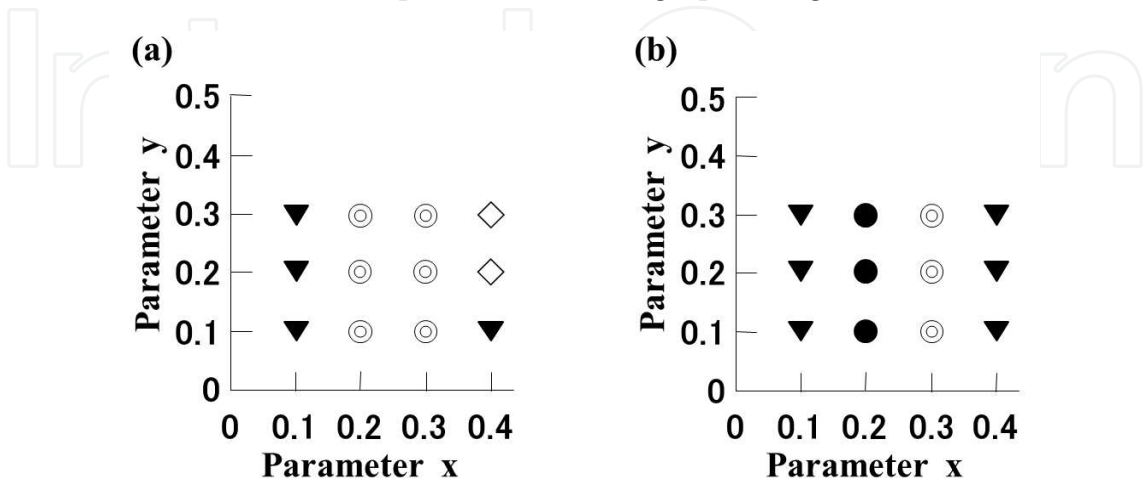

Fig. 14. The diagrams of phase-composition of NYTiS glass-ceramics heated at 900°C (a) and 1000°C (b) for 5 h. ● Na$_5$RSi$_4$O$_{12}$ (N5) ▼ Na$_9$RSi$_6$O$_{18}$ (N9) ◎ N5+N9 ◇ N3+N9

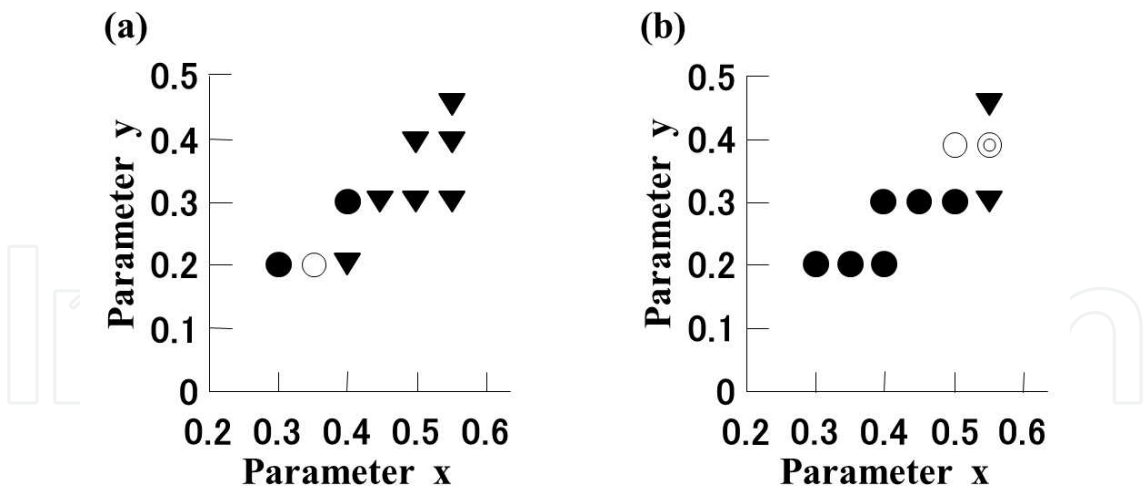Fig. 15. The diagrams of phase-composition of NYGeS glass-ceramics heated at 900°C (a) and 1000°C (b) for 5 h. ● $Na_5RSi_4O_{12}$ (N5) ▼ $Na_9RSi_6O_{18}$ (N9) ○ N5+N3 ◎ N5+N9

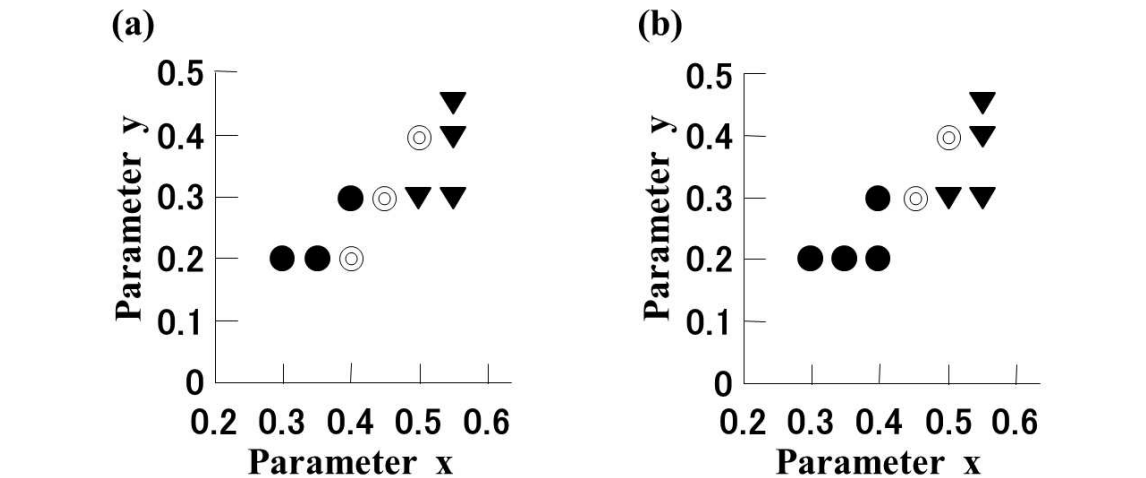Fig. 16. The diagrams of phase-composition of NYTeS glass-ceramics heated at 900°C (a) and 1000°C (b) for 5 h. ● $Na_5RSi_4O_{12}$ (N5) ▼ $Na_9RSi_6O_{18}$ (N9) ◎ N5+N9

| Specimen | Heat-treatment | | σ_{300} | E_a / kJ·mol⁻¹ | | |
	Temp.	Time	/10⁻²·S·cm⁻¹	T	G	GB
NYTiS	1000	5	2.5	15.5	19.8	10.0
NYGeS	900	5	4.0	21.1	17.3	44.0
	1000	5	4.5	24.1	19.3	56.6
	1000	24	6.7	22.9	20.6	67.2
NYTeS	900	5	3.2	19.8	18.7	43.7
	1000	5	4.6	21.8	20.5	56.6

σ_{300} : conductivity at 300°C

E_a : activation energy (T:total G:grain GB:grain boundary)

Table 4. Conduction properties of the N5 glass-ceramics with $Na_{3.6}Y_{0.8}Ti_{0.2}Si_{2.8}O_9$, $Na_{4.2}Y_{0.6}Ge_{0.3}Si_{2.7}O_9$ and $Na_{4.2}Y_{0.6}Te_{0.3}Si_{2.7}O_9$ compositions.

5.2.2 Effect of substitution of Si with V and Mo on ionic conductivity of Na$_5$YSi$_4$O$_{12}$-type glass-ceramics

Glass-ceramics of the vanadium- or molybdenum-containing N5-type Na$^+$-superionic conductors were prepared by crystallization of glasses with the compositions Na$_{3+3x-y}$Y$_{1-x}$V$_y$Si$_{3-y}$O$_9$ (NYVS) or Na$_{3+3x-2y}$Y$_{1-x}$Mo$_y$Si$_{3-y}$O$_9$ (NYMS), and the effects of V or Mo elements on the separation of the phase and the microstructural effects on the conduction properties of glass-ceramics were discussed.

The glass-ceramics have been obtained under the appropriate sets of the parameters x and y of the composition formulas Na$_{3+3x-y}$Y$_{1-x}$V$_y$Si$_{3-y}$O$_9$ or Na$_{3+3x-2y}$Y$_{1-x}$Mo$_y$Si$_{3-y}$O$_9$ ranging in x=0.3~0.5 and y=0.1~0.4. The precursor glasses were made by melting stoichiometric mixtures of reagent-grade powders of anhydrous Na$_2$CO$_3$, Y$_2$O$_3$, V$_2$O$_5$, MoO$_3$ and SiO$_2$ at 1400°C for 1 h, followed by annealing for several hours at an optimum temperature. Shown in Fig. 17 are the diagrams of phase-composition-crystallization temperature of the glass-ceramic specimens with the Na$_{3.9}$Y$_{0.6}$V$_{0.3}$Si$_{2.7}$O$_9$ (A) and Na$_{3.7}$Y$_{0.7}$Mo$_{0.1}$Si$_{2.9}$O$_9$ (B) compositions. N5-type NYVS and NYMS are obtained as a stable phase at high-temperatures. The crystallization of N5 single phase is strongly dependent both on the contents of yttrium and (vanadium or molybdenum) ions (or the values x and y correspond to the composition parameters in Na$_{3+3x-y}$Y$_{1-x}$V$_y$Si$_{3-y}$O$_9$ or Na$_{3+3x-2y}$Y$_{1-x}$Mo$_y$Si$_{3-y}$O$_9$). N3 and N9 phases can be

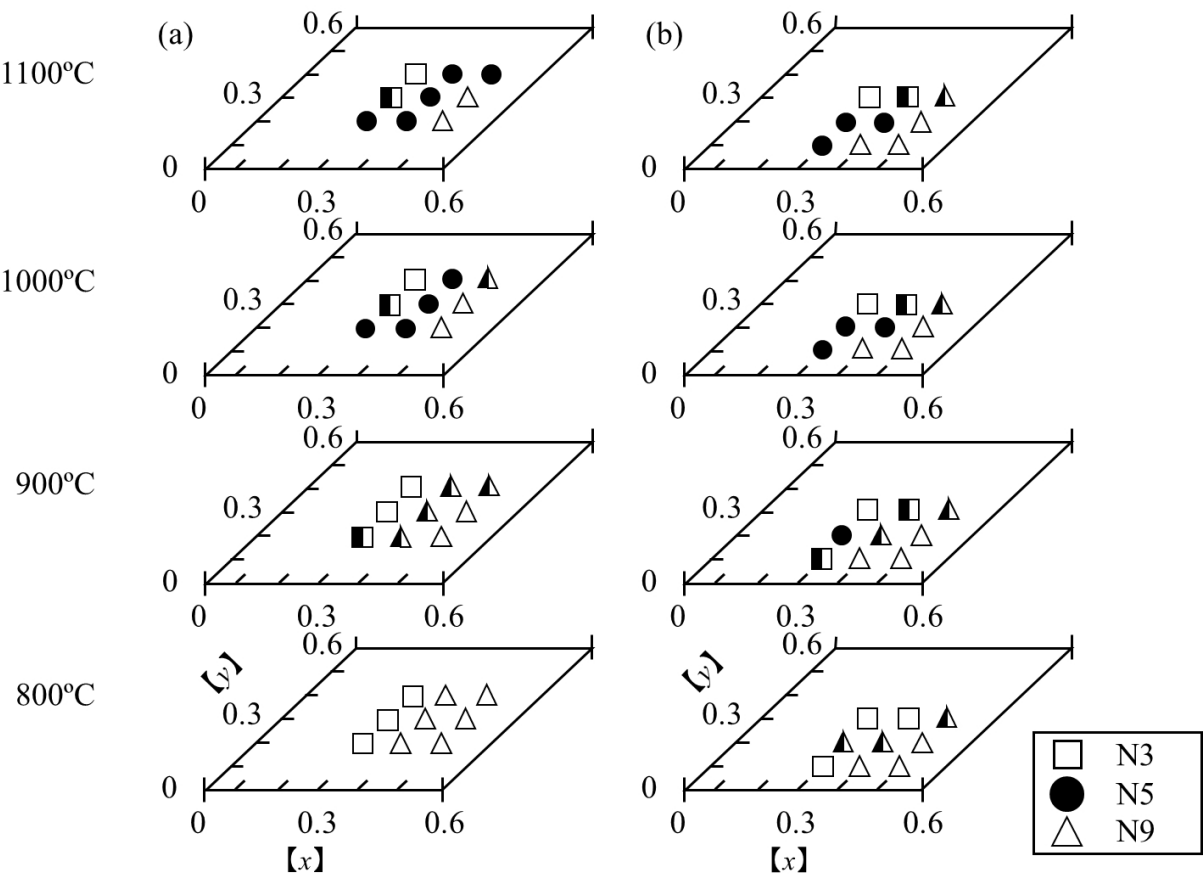
Fig. 17. The diagrams of phase-composition-crystallization temperature of NYVS (a) and NYMS (b) glass-ceramics crystallized at 800~1100°C.
● Na$_5$RSi$_4$O$_{12}$ (N5) □ Na$_3$RSi$_3$O$_9$ (N3) △ Na$_9$RSi$_6$O$_{18}$ (N9) ◧ N5＋N3 ▲ N5＋N9

crystallized as the high-temperature stable phases at the regions of rather lower [Y] and higher [Y], respectively. The total conductivities and the activation energies are summarizes in Table 1. The total conductivities of the specimens (A) and (B) were 0.87×10^{-2} and 3.58×10^{-2} S/cm at 300°C, respectively, and the activation energies of those specimens were 38.1 and 21.8 kJ/mol, respectively. The combination of x and y was most varied in N5-type NYPS and more limited in N5-type NYVS and NYMS. The conductivity decreases giving the order NYPS>NYMS>NYVS. It is considered that this order corresponds to the N5 single phase region. We assume that the effect of the substitution of Si with V or Mo should be to bring about the difference of homogeneity in the N5 ring structure. The total and electronic conductivities and the Na^+ ionic transport numbers of the specimen (A) determined by Wagner polarization method are summarizes in Table 5. The ionic transport numbers of the specimen (A) were nearly 0.9, while those of the specimen (B) were nearly 1. It is considered that about 10% of total conduction is electronic conduction (hopping conduction by transition metal vanadium) in the specimen (A). This result can explain following facts; the conductivity of the specimen (A) are lower than other N5 conductors.

(A)

Temp.	σ / 10^{-1} S·cm^{-1}			E_a / kJ·mol^{-1}		
/ °C	G	GB	T	G	GB	T
150	0.43	0.19	0.13			
200	0.44	0.73	0.28	10.5	47.1	27.5
250	0.62	1.97	0.47			
300	1.24	2.93	0.87	40.5	31.7	38.1
350	2.33	5.38	1.63			

σ : Conductivity E_a : Activation Energy   G: Grain GB: Grain Boundary T: Total

(B)

Temp.	σ / 10^{-1} S·cm^{-1}			E_a / kJ·mol^{-1}		
/ °C	G	GB	T	G	GB	T
150	1.24	1.27	0.63			
200	2.11	4.68	1.45		41.1	29.2
250	3.33	9.45	2.46	22.5		
300	4.81	13.91	3.58		19.1	21.8
350	6.49	15.95	4.61			

σ : Conductivity E_a : Activation Energy   G: Grain GB: Grain Boundary T: Total

Table 5. Total conductivities and activation energies of the glass-ceramic specimens $Na_{3.9}Y_{0.6}V_{0.3}Si_{2.7}O_9$ (A) and $Na_{3.7}Y_{0.7}Mo_{0.1}Si_{2.9}O_9$ (B).

5.3 Structure and conduction properties of $Na_5YSi_4O_{12}$-type glass-ceramics synthesized by bias crystallization of glass

Glass-ceramics of the phosphorus containing N5-type Na^+ superionic conductors were prepared by bias crystallization of glasses with the composition $Na_{4.05}Y_{0.55}P_{0.3}Si_{2.7}O_9$ in an

electric field. The conditions for bias crystallization are discussed with respect to the microstructure and the conduction properties.

The precursor glasses were made by melting stoichiometric mixtures of reagent-grade powders of anhydrous Na_2CO_3, Y_2O_3, SiO_2 and $NH_4H_2PO_4$ at 1350°C for 1h, followed by annealing for several hours at an optimum temperature. The annealed specimens were heated up to 900°C in an electric field for bias crystallization. The thermostable heating holder was produced in order to do the crystallization in a direct current electric field. This holder is made of alumina and platinum. Glass samples (5 mm × 5 mm × 8 mm) were held between the platinum plates, and crystallized in the electrical field using 1 V/mm. The thermal treatment was the same as that used in conventional crystallization in nonelectric field.

The microstructure was investigated with SEM. The grain length of the cross section which is parallel with the electric field direction was 10∼15 nm, and it was proven to be smaller than the 15∼30 nm grain length of the cross section which is perpendicular to the direction and the specimen crystallized by the conventional method. It was possible to control shape and orientation of crystal grain by the crystallization in the electrical field.
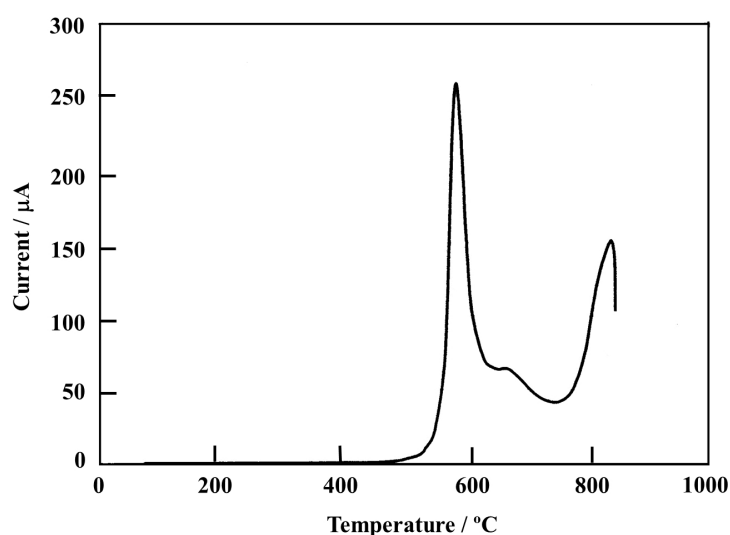

Fig. 18. Current profile in relation to temperature during crystallization process in electric field.

Due to the bias field an electric current in relation to temperature was measured during crystallization process. Fig. 18 shows current profile in relation to temperature during crystallization process in the electric field. The largest observed current was 250 μA. The current profile exhibits three peaks at about 600°C, 700°C and 850°C. These temperatures correspond to those of nucleation, phase transition from N3-phase to N5-phase, and crystallization of glass specimens determined by DTA analysis, respectively. An electric current in relation to temperature was measured newly by applying the bias voltage only in two limited temperature range, because two main peaks were observed in Fig. 18. One range is from right before of the first main peak (511°C to 652°C), and another range is from right before of the second main peak (790°C to 865°C). The resulting current profile is shown in Fig. 19. It was found that the mass transfer in the specimen is being generated even in the condition that does not apply the voltage.
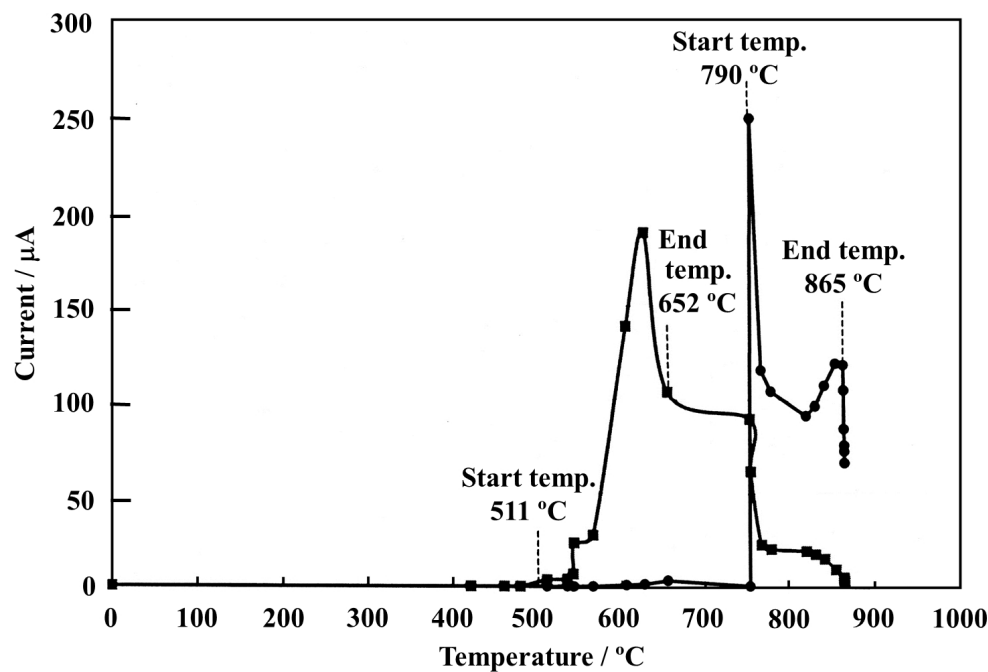
Fig. 19. Current profile in relation to temperature measured by applying voltage in two limited temperature ranges.
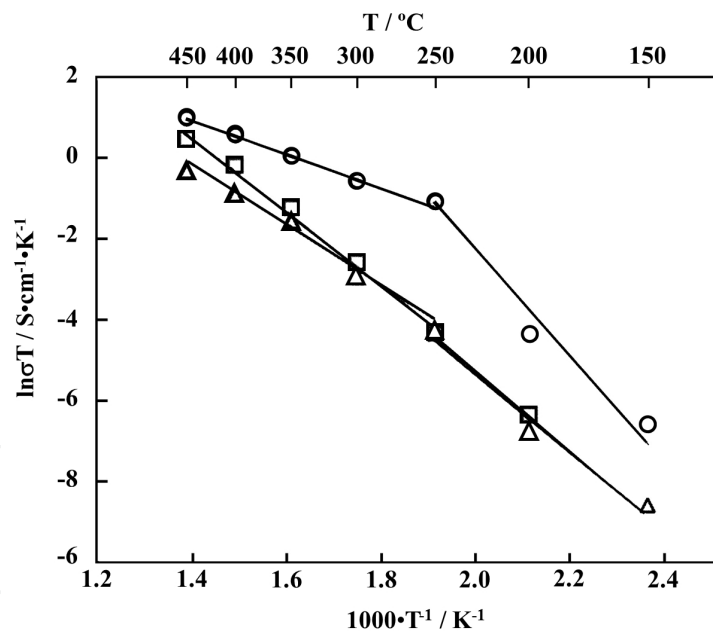

Fig. 20. Temperature dependence Arrhenius plots of the conductivities of the bias crystallized NaRPSi glasses. ◯ Conventional △ Parallel ☐ Perpendicular

Crystalline phases were identified on the sample after the crystallization in the electric field by the X-ray diffraction (XRD) method in order to consider the possibility of structural change by the movement of Na^+ ion which is a carrier. In the several cut sections, no difference in the fundamental structure was observed. Judging from the patterns, the N5 single phase ionic conductors were successfully produced by bias crystallization of glasses.

	E_a / kJ·mol^{-1}		σ_{300}/ mS·cm^{-1}
	Temperature		
	High	**Low**	
○ **Conventional**	33.0	99.9	0.9860
△ **Parallel**	66.6	73.5	0.0923
□ **Perpendicular**	76.4	82.2	0.1320

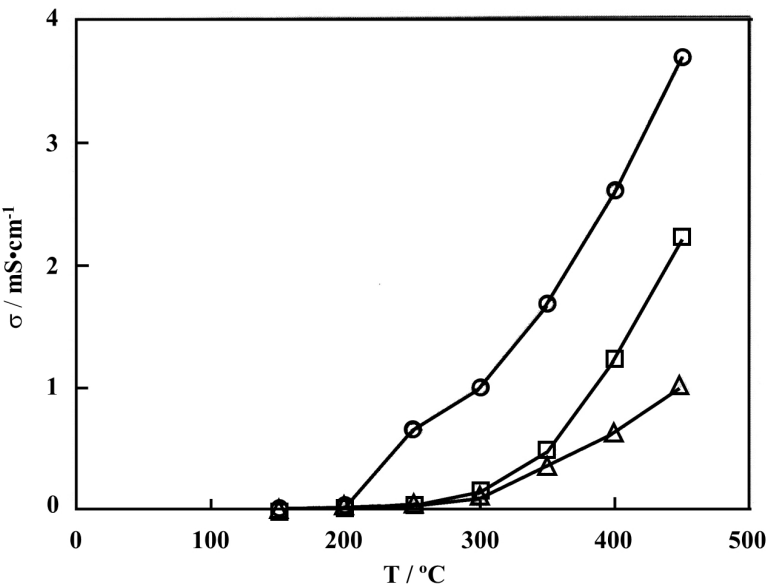Table 6. Conduction properties of the bias-crystallized NaRPSi glasses.

Fig. 21. Temperature dependence of conductivity of the bias crystallized NaRPSi glasses.

Fig. 20 shows the temperature dependence Arrhenius plots of the conductivities of various specimens. The complex admittances of the measured glass-ceramics consisted of two semicircles below 300°C. The two intercepting points on the real axis are interpreted as the resistance of crystallized grains (R_G) and the total resistance of grains and remaining glassy grain boundaries (R_{GB}). As R_{GB} decreases rapidly with increasing temperature because of high (E_a)$_{GB}$ to a comparable value with R_G at 300°C, the total conductivities (R_G+R_{GB}) are dominated by grain boundary conductivity. The effect of the grain boundary is greatly seen on the appearance at lower temperatures. Table 6 summarizes the conduction properties obtained from Fig. 20. The cross sections which are parallel and perpendicular to the electric field direction showed the ionic conductivities of 0.0923 and 0.132 mS/cm at 300°C, respectively. It was found that the bias crystallized specimens were less conductive than that crystallized by the conventional method. Fig. 21 shows the temperature dependence of conductivity of the bias crystallized specimen. In the temperatures over 300°C, anisotropy in the conductivity was observed. It was also found that the cross section which is perpendicular to the electric field direction was more conductive than that in parallel with the direction. The microstructure and the electric conductivity of the NaRPSi glass-ceramics perpendicular to the electric field direction were significantly different from those in parallel.

6. Conclusion

The Na$^+$-superionic conducting glass-ceramics with N5-type structure were successfully produced using the sodium rare earth silicophosphate composition of Na$_{3+3x-y}$R$_{1-x}$P$_y$Si$_{3-y}$O$_9$, in which the rare earth elements of Sc to Sm were applicable to R. The possible combinations of x and y became more limited for the crystallization of the superionic conducting phase as the ionic radius of R increased, while the Na$^+$ conduction properties were more enhanced in the glass-ceramics of larger R. The meaning of the composition formula can be signified in the thermodynamic and kinetic study of crystallization and phase transformation of metastable to stable phase in the production of N5-type glass-ceramics. It was demonstrated that the medium value of content product as [P]×[R] is important in the crystallization of N5 single phase. Conduction properties of these glass-ceramics were strongly dependent upon the crystallization conditions as well as compositions. Not only complex impedance analysis but also TEM observation confirmed that this dependence was attributed to the conduction properties of grain boundaries which were glasses condensed at triple points enclosed by grains.

Glass-ceramics of the N5-type superionic conductors in the system Na$_2$O-Sm$_2$O$_3$-P$_2$O$_5$-SiO$_2$ were prepared by crystallization of glasses with the composition Na$_{3+3x-y}$Sm$_{1-x}$P$_y$Si$_{3-y}$O$_9$. The optimum conditions for crystallization were discussed with reference to the conduction properties and the preparation of crack free N5-type glass-ceramics. The crystallization of the N5 single-phase glass-ceramics was dependent strongly on the concentrations of both [R] and [P] (or x and y in the composition parameters) and the temperature for crystallization of glass specimens. The ionic conductivity of the glass-ceramic Na$_{4.1}$Sm$_{0.5}$P$_{0.4}$Si$_{2.6}$O$_9$ was 4.78×10^{-2} S/cm at 300°C. The grain size of the specimen was about 3-5 μm. The state of grain growth is promoted with increase of heating temperature and heating time for crystallization. Although grain growth may cause high conductivity, it was difficult to prevent the sample heated for a long time from cracking during crystallization.

Glass-ceramics of the titanium-, germanium- or tellurium-containing N5-type superionic conductors were prepared by crystallization of glasses with the composition Na$_{3+3x}$Y$_{1-x}$X$_y$Si$_{3-y}$O$_9$ (X=Ti, Ge, Te), and the effects of X elements on the separation of the phase and the microstructural effects on the conduction properties of glass-ceramics were discussed. The combination of x and y was most varied in N5YGeS and more limited in the order of N5YTeS>N5YTiS. Their conductivities and activation energies are of the order of 10^{-2} S/cm at 300°C and of 15 to 24 kJ/mol, respectively. The conductivity of the glass-ceramic N5YXS decreases giving the order N5YGeS>N5YTeS>N5YTiS. It is considered that this order corresponds to the N5 single phase region. Large enhancement of electrical conductivity was observed in the glass-ceramics as the grain growth was promoted with increase of heating temperature and heating time for crystallization.

Glass-ceramics of the vanadium- or molybdenum-containing N5-type superionic conductors were prepared by crystallization of glasses with the compositions Na$_{3+3x-y}$Y$_{1-x}$V$_y$Si$_{3-y}$O$_9$ or Na$_{3+3x-2y}$Y$_{1-x}$Mo$_y$Si$_{3-y}$O$_9$. The combination of x and y was most varied in N5-type NYPS and more limited in N5-type NYVS and NYMS. The conductivities of the glass-ceramic specimens with the Na$_{3.9}$Y$_{0.6}$V$_{0.3}$Si$_{2.7}$O$_9$ (A) and Na$_{3.7}$Y$_{0.7}$Mo$_{0.1}$Si$_{2.9}$O$_9$ (B) compositions were 0.87×10^{-2} and 3.58×10^{-2} S/cm at 300°C, respectively. The conductivity decreases giving the order NYPS>NYMS>NYVS. It is considered that this order corresponds to the N5 single phase region. We assume that the effect of the substitution of Si with V or Mo should be to bring about the difference of homogeneity in the N5 ring structure. The Na$^+$ ionic transport

numbers of these glass-ceramics determined by Wagner polarization method were nearly 0.9 for the specimen (A) and 1 for the specimen (B) at 300°C, respectively. It is considered that about 10% of total conduction is electronic conduction in the specimen (A). This result can explain following facts; the conductivity of the specimen (A) are lower than other N5 conductors, and it is seen in the temperature dependence Arrhenius plots for the specimen (A) that the lines drawn from the conductivity of grains are bending upwards.

We have successfully produced the N5-type glass-ceramic conductors by bias crystallization of the glasses with the composition $Na_{4.05}Y_{0.55}P_{0.3}Si_{2.7}O_9$ in an electric field. The microstructure and the conduction properties were dependent on the current direction in the process of crystallization. The cross sections which are parallel and perpendicular to the electric field direction showed the ionic conductivities of 0.0923 and 0.132 mS/cm at 300°C, respectively. The microstructure and the electric conductivity of the glass-ceramics perpendicular to the electric field direction were significantly different from those in parallel.

7. Acknowledgment

8. References

Alexander, M. G. (1987). Effect of modifier cations on Na⁺ conductivity in sodium silicate glasses. *Solid State Ionics*, 22, 257.

Banks, E. & Kim. C. H. (1985). Ionic conductivity in glass and glass-ceramics of the $Na_3YSi_3O_9$ and $Na_5YSi_4O_{12}$ type materials. *J. Electrochem. Soc.*, 132, 2617-2621.

Beyeler, H. U. & Himba, T. (1978). The sodium conductivity paths in the superionic conductors $Na_5RESi_4O_{12}$. *Solid State Commun.*, 27, 641-643.

Beyeler, H. U.; Shannon, R. D. & Chen H. Y. (1980). Ionic conductivity of single-crystal $Na_5YSi_4O_{12}$. *Appl. Phys. Lett.*, 37, 934-936.

Cervantes, F.; Marr, L. J. & Glasser, F. P. (1981). Compounds in the $Na_2O-Y_2O_3-SiO_2$ system. *Ceram. Intl.*, 7(2), 43-47.

Hong, H. Y-P.; Kafalas, J. A. & Bayard, M. (1978). High Na⁺-ion conductivity in $Na_5YSi_4O_{12}$. *Mater. Res. Bull.*, 13, 757-761.

Kim, C. H.; Qiu, B. & Banks, E. Ionic conductivity in solid solutions of the $Na_3YSi_3O_9$ type. (1985). *J. Electrochem. Soc.*, 132, 1340-1345.

Kingery, W. D.; Bowen, H. K. & D. R. Uhlmann. (1976). *Introduction to Ceramics, 2nd ed.*, John Wiley & Sons, Inc., New York, p. 368-369.

Maksimov, B. A.; Petrov, I. V.; Rabenau, A. & Schulz, H. (1982). X-ray investigations and possible mechanism for the ionic conductivity in the $Na_5RESi_4O_{12}$ (RE=Y, Sc) class of compounds. *Solid State Ionics*, 6, 195-200.

Morimoto, S. (1989). Ionic conductivity of $Na_2O-ZrO_2-P_2O_5-SiO_2$ system glass ceramic. *J. Ceram. Soc. Jpn.*, 97, 1097-1103.

Okura, T.; Tanaka, M.; Kanzawa, H. & Sudoh, G. (1996). Synthesis and conduction properties of Na⁺ superionic conductors of sodium samarium silicophosphates. *Solid State Ionics*, 86-88, 511-516.

Okura, T.; Yamashita, K. & Umegaki, T. (1996). Na⁺-ion conduction properties of glass-ceramic Narpsio in the Y-Sm mixed system. *Phosphorus Research Bulletin*, 6, 237-240.

Okura, T.; Tanaka, M. & Sudoh, G. (1997). Conduction properties of Na^+-ion implanted glass-ceramics in the system $Na_2O-R_2O_3P_2O_5-SiO_2$ (R = rare earth). *Mat. Res. Soc. Symp. Proc.*, Vol. 453, 611-616.

Okura, T. & Yamashita, K. (2000). Ionic conductivities of Na^+-ion implanted silico-phosphate glass-ceramics. *Solid State Ionics*, 136-137, 1049-1054.

Okura, T.; Inami, Y.; Monma, H.; Nakamura, S. & Yamashita. K. (2002). Structure and conduction properties of Na^+ superionic conductor Narpsio synthesized by bias crystallization of glass. *Solid State Ionics*, 154-155, 361-366.

Okura, T.; Tanaka, M.; Monma, H.; Yamashita, K. & Sudoh, G. (2003). New superionic conducting glass-ceramics in the system $Na_2O-Y_2O_3-Sm_2O_3-P_2O_5-SiO_2$: crystallization and ionic conductivity. *J. Ceram. Soc. Jpn.*, 111/4, 257-261.

Okura, T.; Monma, H. & K. Yamashita. (2004). Na^+-superionic conductors of glass-ceramics in the system $Na_2O-Sm_2O_3-X_2O_3-P_2O_5-SiO_2$ (X=Al, Ga). *Solid State Ionics*, 172, 561-564.

Okura, T.; Monma, H. & Yamashita, K. (2004). Effect of substitution of Si with Ge and Te on ionic conductivity of $Na_5SmSi_4O_{12}$–type glass-ceramics. *J. Ceram. Soc. Jpn.*, 112/ 5, S685-S689.

Okura, T.; Monma, H. & Yamashita, K. (2006). Superionic conducting $Na_5SmSi_4O_{12}$-type glass-ceramics: Crystallization condition and ionic conductivity. *J. Eur. Ceram. Soc.*, 26, 619.

Okura, T.; Takahashi, T; Monma, H. & Yamashita. K. Effect of substitution of Si with V and Mo on ionic conductivity of $Na_5YSi_4O_{12}$–type glass-ceramics. (2008). *Solid State Ionics*, 179, 1291-1295.

Okura, T.; Saimaru, M; Monma, H. & Yamashita. K. (2009). Ionic conductivities of Nasicon-type glass-ceramic superionic conductors in the system $Na_2O-Y_2O_3-XO_2-SiO_2$ (X=Ti, Ge, Te). *Solid State Ionics*, 180, 537-540.

Okura, T; Monma, H & Yamashita, K. (2010). Na^+-fast ionic conducting glass-ceramics of silicophosphates. *J. Electroceram.*, 24, 83-90.

Shannon, R. D.; Taylor, B. E.; Gier, T. E.; Chen, H. Y. & Berzins, T. (1978). Ionic conductivity in $Na_5YSi_4O_{12}$–type silicates. *Inorg. Chem.*, 17, 958-964.

Shannon, R. D.; Gier, T. E.; Foris, C. M.; Nelen, J. A. & Appleman, D. E. (1980). Crystal data for some sodium rare earth silicates. *Phys. Chem. Minerals*, 5, 245-253.

Yamashita, K.; Ohkura, S.; Umegaki, T. & Kanazawa, T. (1988). Synthesis and ionic conduction of C_3A-type Nasicon $Na_{3+3x-y}Y_{1-x}Si_{3-y}P_yO_9$. *Solid State Ionics*, 26, 279-286.

Yamashita, K.; Ohkura, S.; Umegaki, T. & Kanazawa, T. (1988). Synthesis, polymorphs and sodium ionic conductivity of sodium yttrium silicophosphates with the composition $Na_{3+3x-y}Y_{1-x}P_ySi_{3-y}O_9$. *J. Ceram. Soc. Jpn.*, 96, 967-972.

Yamashita, K.; Nojiri, T.; Umegaki, T. & Kanazawa, T. (1989). New fast sodium-ion conducting glass-ceramics of silicophosphates: Crystallization, microstructure and conduction properties. *Solid State Ionics*, 35, 299-306.

Yamashita, K.; Nojiri, T.; Umegaki, T. & Kanazawa, T. (1990). Na^+ superionic conductors of glass-ceramics in the system $Na_2O-Re_2O_3-P_2O_5-SiO_2$ (Re=rare-earth elements). *Solid State Ionics*, 40/41, 48-52.

Yamashita, K.; Tanaka, M. & Umegaki, T. (1992). Thermodynamic and kinetic study on the phase transformation of the glass-ceramic Na^+ superionic conductors $Na_{3+3x-y}Re_{1-x}P_ySi_{3-y}O_9$. *Solid State Ionics*, 58, 231-236.

Yamashita, K.; Tanaka, M.; Kakuta, T.; Matsuda, M. & Umegaki, T. (1993). Effects of rare earth elements on the crystallization of the glass-ceramic Na^+ superionic conductor Narpsio-V. *J. Alloys and Compounds*, 193, 283-285.

Yamashita, K.; Umegaki, T.; Tanaka, M.; Kakuta, T. & Nojiri, T. (1996). Microstructural effects on conduction properties of $Na_5YSi_4O_{12}$-type glass-ceramic Na^+-fast ionic conductors. *J. Electrochem. Soc.*, 143, 2180-2186.
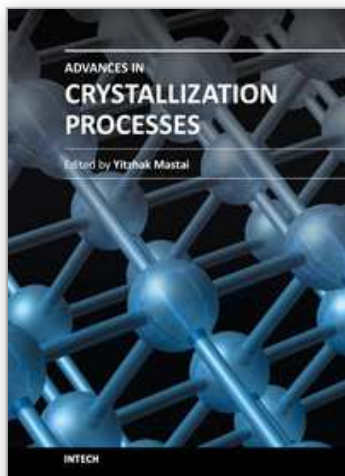
Advances in Crystallization Processes
Edited by Dr. Yitzhak Mastai

Crystallization is used at some stage in nearly all process industries as a method of production, purification or recovery of solid materials. In recent years, a number of new applications have also come to rely on crystallization processes such as the crystallization of nano and amorphous materials. The articles for this book have been contributed by the most respected researchers in this area and cover the frontier areas of research and developments in crystallization processes. Divided into five parts this book provides the latest research developments in many aspects of crystallization including: chiral crystallization, crystallization of nanomaterials and the crystallization of amorphous and glassy materials. This book is of interest to both fundamental research and also to practicing scientists and will prove invaluable to all chemical engineers and industrial chemists in the process industries as well as crystallization workers and students in industry and academia.

INTECH
open science | open minds